EPI International Journal of Engineering
Volume 9, Number 1, February 2026, pp. 71-81
DOI: 10.25042/epi-ije.022026.10

*p*ISSN 2615-5109
*e*ISSN 2621-0541

The In-plane Vibration of Free, Supported and Clamped Circular Plates

Yoshihiro Narita*,[a]

[a]Faculty of Engineering, Hokkaido University (Professor Emeritus), Japan, Email: ynarita1951@gmail.com

Abstract

Only a limited number of numerical studies have addressed the in-plane vibration of solid circular plates. This contrasts with the bending vibration of circular plates, for which closed-form solutions in terms of Bessel functions exist and natural frequency data are widely available in the literature for the three classical boundary conditions: free, simply supported, and clamped edges. In the present work, an effective method based on a previously established Ritz approach in polar coordinates is developed to calculate the in-plane natural frequencies of solid circular plates. Extensive and accurate frequency parameters are presented for four types of in-plane boundary conditions: free, S-1 type support, S-2 type support, and clamped edges. For each boundary condition, tables are provided covering Poisson's ratios $\nu = 0$, 0.1, 0.2, 0.3, 0.4, 0.5, as well as $\nu = 0.333$. The influence of boundary conditions and Poisson's ratio on the in-plane vibration characteristics of circular plates is thus systematically investigated and clarified.

Keywords: Circular plate, in-plane vibration, boundary condition, natural frequency, Ritz method

1. Introduction

Free vibration of solid circular plates (i.e., with no holes) has been of academic and technical interest for a long time [1]. In particular, the bending (out-of-plane) vibration of circular plates has been well documented for cases in which the outer boundary is subject to classical boundary conditions. Natural frequency data are available for completely free plates [2], simply supported plates [3], and clamped plates [4].

Flat plates exhibit two distinct types of vibration: bending vibration and in-plane vibration. As noted above, bending vibration has been studied extensively, whereas in-plane vibration has received sparse attention. Nevertheless, there is clearly a technical need for organized and reliable datasets of in-plane natural frequencies for plates with regular geometries, such as solid circular plates.

In-plane vibration of annular plates with concentric inner and outer circular boundaries has been investigated by a number of authors [5–10], largely because the presence of an inner boundary avoids the singularity at the plate center (for example, in the integration of strain energy). Irie et al. [5] employed the transfer matrix method in 1984 to obtain in-plane natural frequencies of annular plates with free or clamped boundaries. More recently, during the 2010s, several studies [6–9] applied analytical methods, the finite element method, and other approximate approaches. An updated list of related references can be found in [10].

For *solid* circular plates (i.e., plate with no central hole), however, only a limited number of studies on in-plane vibration are available. Existing works primarily address clamped or elastically restrained boundary conditions. Farag and Pan [11] investigated the in-plane modal characteristics of clamped solid circular plates, while Park [12] derived the corresponding frequency equations. Kim et al. [13] considered elastically restrained plates. Nevertheless, comprehensive numerical data for in-plane vibration of solid circular plates under various boundary conditions—including free edges and different types of supported edges—remain scarce.

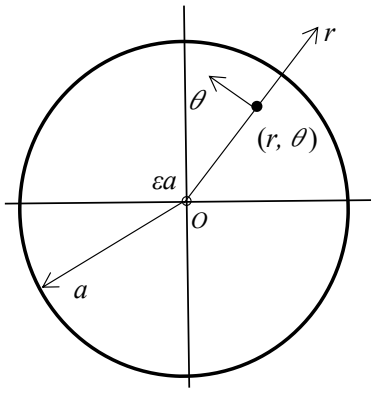


Figure 1. Circular plate with an infinitesimal hole in the center and co-ordinate system

*Corresponding author.
Hokkaido University, N-13, W-8, Sapporo
Japan

The purpose of the present work is therefore to provide accurate and extensive numerical results for the in-plane natural frequencies of solid circular plates with typical edge conditions and different Poisson's ratios. These results are intended to serve as a useful reference for both designers and researchers.

2. Method of analysis

2.1 Energy formulation

Free in-plane vibration of a circular plate with a central hole of infinitesimal size is analyzed in the polar coordinates, as shown in Fig. 1. Outer and inner radii are given by a and εa, respectively, and the uniform thickness is h. The inner boundary is assumed to be free edge, and the ε represents an extremely small parameter to simulate a solid circular plate. The plate is subjected to any in-plane boundary condition along the outer edge.

Assuming sinusoidal time variation in radian frequency ω, the maximum in-plane strain energy of the plate is expressed in the form of

$$U = \frac{1}{2}\int_{\varepsilon a}^{a}\int_{0}^{2\pi}\{\bar{\varepsilon}\}^{T}[A]\{\bar{\varepsilon}\}\,rd\theta dr \tag{1}$$

where $\{\bar{\varepsilon}\}$ is the strain vector and [A] is in-plane stiffness matrix:

$$\{\bar{\varepsilon}\}=\begin{Bmatrix}\dfrac{\partial u}{\partial r}\\ \dfrac{1}{r}\left(u+\dfrac{\partial v}{\partial \theta}\right)\\ \dfrac{1}{r}\left(\dfrac{\partial u}{\partial \theta}-v\right)+\dfrac{\partial v}{\partial r}\end{Bmatrix},\quad [A]=\begin{bmatrix}A_r & \nu_\theta A_r & 0\\ \nu_\theta A_r & A_\theta & 0\\ 0 & 0 & A_k\end{bmatrix} \tag{2}$$

where $u(r,\theta)$ and $v(r,\theta)$ are the in-plane amplitudes of plate in the radial and circumferential direction, respectively. The maximum in-plane kinetic energy of the plate is

$$T = \frac{1}{2}\rho h\omega^2\int_{\varepsilon a}^{a}\int_{0}^{2\pi}\left(u^2+v^2\right)rd\theta dr \tag{3}$$

For polar-orthotropic material, a set of the in-plane stiffness is defined by

$$A_r=\frac{E_r h}{1-\nu_r\nu_\theta},\ A_\theta=\frac{E_\theta h}{1-\nu_r\nu_\theta},\ A_k=G_{r\theta}h \tag{4}$$

where E_r and E_θ are Young's moduli in r and θ direction, respectively, $G_{r\theta}$ is a shear modulus, ν_r and ν_θ are Poisson's ratios ($\nu_\theta A_r=\nu_r A_\theta$), and ρ is the averaged mass of plate per unit volume. For isotropic material, equations (4) reduce to

$$A_r=A_\theta=\frac{Eh}{1-\nu^2},\quad H=A_r\nu_\theta+2A_k=\frac{Eh}{1-\nu^2} \tag{5}$$

where H is a combined stiffness.

Separation of variables is assumed as

$$u(r,\theta)=U(r)\cos n\theta,\quad v(r,\theta)=V(r)\sin n\theta \tag{6}$$

where $U(r)$ and $V(r)$ are functions of r in the radial direction and n is an integer to prescribe the number of nodal diameters. Equations (6) are substituted into Eq.(1) and by integrating over θ in the circumferential direction, one gets

$$U=\frac{\pi}{2}\int_{\varepsilon a}^{a}\{\bar{\varepsilon}\}^{T}[A]\{\bar{\varepsilon}\}\,rdr \tag{7}$$

where the strain vector becomes

$$\{\bar{\varepsilon}\}=\begin{Bmatrix}\dfrac{dU}{dr}\\ \dfrac{1}{r}(U+nV)\\ -\dfrac{1}{r}(nU+V)+\dfrac{dV}{dr}\end{Bmatrix} \tag{8}$$

Similarly, equation (3) becomes

$$T=\frac{\pi}{2}\rho h\omega^2\int_{\varepsilon a}^{a}\left(U^2+V^2\right)rdr \tag{9}$$

The resulting functional is given for the problem by

$$F=T-U \tag{10}$$

2.2 Ritz formulation

For simplicity of analysis, the following variables are introduced in non-dimensional form as

$$\eta=r/a\ \ (\text{non-dimensional radial coordinate}),\qquad \Omega=\omega a\sqrt{\rho\left(1-\nu^2\right)/E}\ \ \begin{pmatrix}\text{frequency parameter}\\ \text{for isotropic plate}\end{pmatrix} \tag{11}$$

As widely known, it is important in the Ritz method to introduce effective trial functions to model the vibrating displacement (amplitude). The functions $U(r)$ and $V(r)$ in Eqs. (6) are assumed by

$$U(\eta)=\sum_{i=0}^{M-1}U_i\eta^i(\eta-1)^{Bu}$$
$$V(\eta)=\sum_{j=0}^{M-1}V_j\eta^j(\eta-1)^{Bv} \tag{12}$$
$$(U_i,V_j:\text{unknown coefficients})$$

where the polynomial functions have the boundary index Bu and Bv to satisfy the kinematical boundary conditions.

Figure 2 illustrates four types of in-plane boundary conditions applied uniformly along the outer edge, and the inner edge at a tiny hole is already set free in Eqs.(12). First example is "Free plate" where both u and v are un-constrained (Bu=Bv=0) at the outer edge. Simply supported plates may be classified into two types with respect to in-plane motion. "S1 supported" is a case where radial displacement is free (Bu=0) but circumferential displacement is set as zero (Bv=1). Instead, "S2 supported" is that radial displacement is constrained as zero (Bu=1) but circumferential displacement is free (Bv=0). It is clear

in "Clamped" plate to make both displacements zero (*Bu*=*Bv*=1).

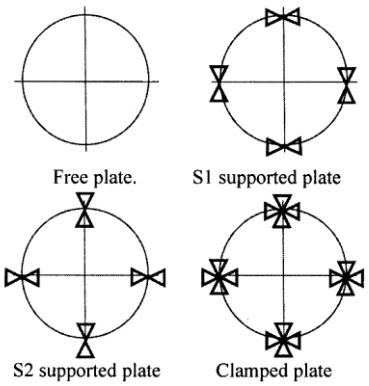


Figure 2. Four types of in-plane boundary conditions of solid circular plate at the outer edge (constraint symbols apply uniformly along the entire edge)

A frequency equation is derived by applying the Ritz process to extremize the functional (10)

$$\frac{\partial F}{\partial U_{\bar{i}}}=\frac{\partial F}{\partial V_{\bar{j}}}=0 \quad \left(\bar{i},\bar{j}=0,1,2,...,M-1\right) \tag{13}$$

with respect to unknown coefficients, and the frequency equation is derived for a specific *n* as

$$\begin{bmatrix} \sum_{i=0}^{M-1} F_{11} & \sum_{j=0}^{M-1} F_{12} \\ sym & \sum_{j=0}^{M-1} F_{22} \end{bmatrix} \begin{Bmatrix} U_i \\ V_j \end{Bmatrix} = 0 \tag{14}$$
$$\left(\bar{i},\bar{j}=0,1,2,...,M-1\right)$$

where

$$\begin{aligned} F_{11} &= a_{11}I_{1,i\bar{i}}^{(11)}+a_{12}\left(I_{0,i\bar{i}}^{(10)}+I_{0,i\bar{i}}^{(01)}\right) \\ &\quad +a_{22}I_{-1,i\bar{i}}^{(00)}+a_{66}n^2I_{-1,i\bar{i}}^{(00)}-\Omega^2I_{1,i\bar{i}}^{(00)} \\ F_{12} &= n\left\{a_{12}I_{0,j\bar{i}}^{(01)}+a_{22}I_{-1,j\bar{i}}^{(00)}\right. \\ &\quad \left.+a_{66}\left(I_{-1,j\bar{i}}^{(00)}-I_{0,j\bar{i}}^{(10)}\right)\right\} \\ F_{22} &= a_{22}n^2I_{-1,j\bar{j}}^{(00)}+a_{66}\left(I_{-1,j\bar{j}}^{(00)}+I_{1,j\bar{j}}^{(11)}\right. \\ &\quad \left.-I_{0,j\bar{j}}^{(10)}-I_{0,j\bar{j}}^{(01)}\right)-\Omega^2I_{1,j\bar{j}}^{(00)} \end{aligned} \tag{15}$$

with

$$\begin{aligned} I_{k,i\bar{i}}^{(pq)} &= \int_{\varepsilon}^{1}\eta^k\frac{d^{(p)}U(\eta,i)}{d\eta^{(p)}}\frac{d^{(q)}U(\eta,\bar{i})}{d\eta^{(q)}}d\eta, \\ I_{k,j\bar{i}}^{(pq)} &= \int_{\varepsilon}^{1}\eta^k\frac{d^{(p)}V(\eta,j)}{d\eta^{(p)}}\frac{d^{(q)}U(\eta,\bar{i})}{d\eta^{(q)}}d\eta, \\ I_{k,j\bar{j}}^{(pq)} &= \int_{\varepsilon}^{1}\eta^k\frac{d^{(p)}V(\eta,j)}{d\eta^{(p)}}\frac{d^{(q)}V(\eta,\bar{j})}{d\eta^{(q)}}d\eta \end{aligned} \tag{16}$$

Integration is carried out in the exact manner (not by using numerical integration) and the eigenvalues are extracted with the help of the eigenvalue subroutine.

2.3 Finite element formulation

The present finite element formulation is based on the same linear elastic theory as in Eq.(1). A pair of in-plane amplitudes are assumed in *r* and θ directions, after having assumed sinusoidal time variation, in

$$\begin{Bmatrix} U(r) \\ V(r) \end{Bmatrix} = [P]\{\beta\} \tag{17}$$

where

$$[P]=\begin{bmatrix} 1 & 0 & r & 0 \\ 0 & 1 & 0 & r \end{bmatrix},\ \{\beta\}=\{\beta_0,\gamma_0,\beta_1,\gamma_1\}^T \tag{18}$$

By assuming one-dimensional element with specified coordinates $r=r_i$ and $r=r_j$ at two nodes ($r_i<r_j$), the element displacement vector at the two nodes is given by

$$\{d_e\}=\{u_i,v_i,u_j,v_j\}^T \tag{19}$$

Substitution of equation (19) into the coordinates at two nodes of the one-dimensional element yields

$$\{d_e\}=[C]\{\beta\},\ \text{i.e.,}\ \{\beta\}=[C]^{-1}\{d_e\} \tag{20}$$

where

$$[C]=\begin{bmatrix} 1 & 0 & r_i & 0 \\ 0 & 1 & 0 & r_i \\ 1 & 0 & r_j & 0 \\ 0 & 1 & 0 & r_j \end{bmatrix} \tag{21}$$

A strain vector in equation (8) is written in the form

$$\{\bar{\varepsilon}\}=[Q]\{\beta\}=[Q][C]^{-1}\{d_e\} \tag{22}$$

An element strain vector is obtained by substituting Eq.(22) into (7) as

$$U_e=\frac{1}{2}\{d_e\}^T[K_e]\{d_e\} \tag{23}$$

where $[K_e]$ is an element stiffness matrix

$$[K_e]=\left([C]^{-1}\right)^T\cdot\int_{ri}^{rj}[Q]^T[A][Q]dr\ \cdot[C]^{-1} \tag{24}$$

In a similar way, an element mass matrix is derived as

$$T_e=\frac{1}{2}\rho h\omega^2\{d_e\}^T[M_e]\{d_e\} \tag{25}$$

where ω is a radian frequency, and $[M_e]$ is an element mass stiffness matrix

$$[M_e]=\left([C]^{-1}\right)^T\cdot\int_{ri}^{rj}\left(U^2+V^2\right)dr\ \cdot[C]^{-1} \tag{26}$$

These element stiffness and mass matrices are embedded in the global system, and then the global system is assembled as

$$\left(\left[K\right]-\rho h\omega^2\left[M\right]\right)\{\delta\}=0 \tag{27}$$

where [*K*], [*M*] and {δ} are global stiffness matrix, global mass matrix and global displacement vector, respectively. As in the Ritz method, eigenvalues ω^2 are extracted from this equation and the radian frequency is modified by Eq.(11) to a dimensionless frequency parameter Ω .

3. Numerical results

When the Ritz method is used in the computation, it is important to test convergence characteristics of frequency parameter Ω by increasing the number of terms *i* and *j* in Eq.(12). Table 1 presents a convergence test for the lowest five frequency parameters Ω_1–Ω_5, reported to the four significant figures for four different boundary conditions. The symbols n and s in (n, s) denote the numbers of nodal diameters and nodal circles, respectively. It can be seen frequency values converge within four significant figures, and identical converged values are underlined. All subsequent results are obtained using *M* = 8 terms.

Table 1 Convergence of in-plane frequency parameters $\Omega=\omega a(\rho(1-\nu^2)/E)^{1/2}$ of circular plates (ν=0.3)

BC	Num.term	Ω_1	Ω_2	Ω_3	Ω_4	Ω_5
Free		(2,0)	(1,1)	(0,1)	(3,0)	(2,1)
	6	1.388	1.618	2.049	2.130	2.511
	7	1.388	1.618	2.049	2.130	2.511
	8	1.388	1.618	2.049	2.130	2.511
	9	1.388	1.618	2.049	2.130	2.511
S1 supported		(1,0)	(2,0)	(0,0)	(3,0)	(0,1)
	6	0.6839	1.432	2.049	2.131	2.267
	7	0.6839	1.432	2.049	2.131	2.267
	8	0.6839	1.432	2.049	2.131	2.267
	9	0.6839	1.432	2.049	2.131	2.267
S2 supported		(1,0)	(1,1)	(2,0)	(0,1)	(2,1)
	6	1.309	2.046	2.482	3.038	3.048
	7	1.309	2.046	2.482	3.038	3.047
	8	1.309	2.046	2.482	3.038	3.047
	9	1.309	2.046	2.482	3.038	3.047
Clamped		(1,0)	(0,0)	(2,0)	(1,1)	(0,1)
	6	1.957	2.267	3.047	3.178	3.832
	7	1.957	2.267	3.047	3.178	3.832
	8	1.957	2.267	3.047	3.178	3.832
	9	1.957	2.267	3.047	3.178	3.832

Table 2 Comparison of frequency parameters $\Omega=\omega a(\rho(1-\nu^2)/E)^{1/2}$

BC	Num.elt.	Ω_1	Ω_2	Ω_3	Ω_4	Ω_5
Free		(2,0)	(1,1)	(0,1)	(3,0)	(2,1)
(ν =0.3)	Ritz	1.388	1.618	2.049	2.130	2.511
	FEM	1.388	1.618	2.049	2.131	2.512
	Irie [5]	1.387	1.618	2.049	2.131	2.511
	Kim [13]	1.3877	1.6176	2.0489	2.1304	2.5112
Clamped		(1,0)	(0,0)	(2,0)	(1,1)	(0,1)
(ν =0.3)	Riz	1.957	2.267	3.047	3.178	3.832
	FEM	1.957	2.267	3.048	3.180	3.832
	Irie [5]	1.958	2.267	3.046	3.180	3.831
(ν =0.33)	Riz	1.944	2.218	3.018	3.113	3.832
	FEM	1.944	2.218	3.019	3.114	3.382
	Park [12]	1.944	2.218	3.018	3.113	3.832

Since this paper aims to compute the natural frequencies of in-plane vibration of solid circular plates and to provide comprehensive and accurate data tables, it is essentially important to numerically verify a fundamental assumption of the analysis—namely, that accurate frequency values can be obtained by modeling a solid circular plate as one with an infinitesimally small central hole.

Figure 3 shows the variation of the frequency parameter Ω as the aspect ratio ε = (inner radius)/(outer radius) decreases from 0.2 to 0.001. Two cases are considered: (a) an S-1 supported circular plate and (b) a clamped circular plate. The frequency values given in the figure correspond to Ω rounded to four significant figures at each data point. The pairs (n, s) shown in squares on the right-hand side denote the numbers of nodal diameters and nodal circles, consistent with those in Tables 1 and 2.

As ε approaches zero—particularly at ε = 0.01 and 0.001—both sets of frequencies converge and take nearly identical values. Based on these results, ε = 0.001 (i.e., a central-hole radius equal to 0.1 % of the outer radius) is adopted hereafter to model solid circular plates in the tabulated results. It is noted that the assumed function (12) is available to the plate with a relatively large (e.g., ε = 0.2) free edge hole.

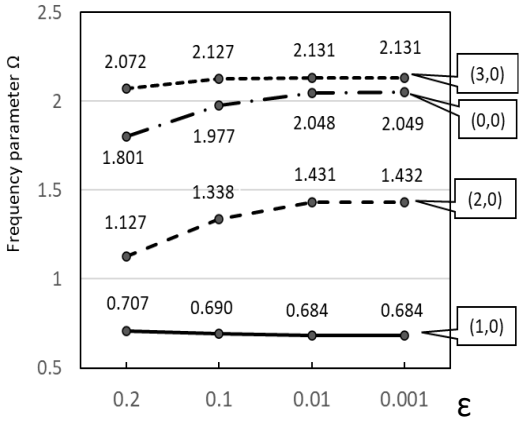
Table 2 compares the frequency parameters obtained by the present Ritz and FEM methods based on the present solid-plate approximation with those reported by Irie et al. [5], Park [12], and Kim et al. [13]. Irie et al. employed the same approximation, whereas the latter two studies derived solutions strictly for solid circular plates. The present results for free and clamped plates show excellent agreement with these published data.

Table 3 tabulates the frequency parameter Ω for "completely free" circular plates, in which both in-plane displacements *u* and *v* are unconstrained at the outer edge. Calculations were performed for n = 0, 1,.., 5 and s = 0, 1, 2, and for seven Poisson's ratios: 0, 0.1, 0.2, 0.3, 0.4, 0.5, and 0.333. The reason why a specific value of 0.333 is included is that this value is quite often used for Aluminum material. All the frequency values obtained using the present Ritz method are compared with those computed using a finite-element program developed by the author.

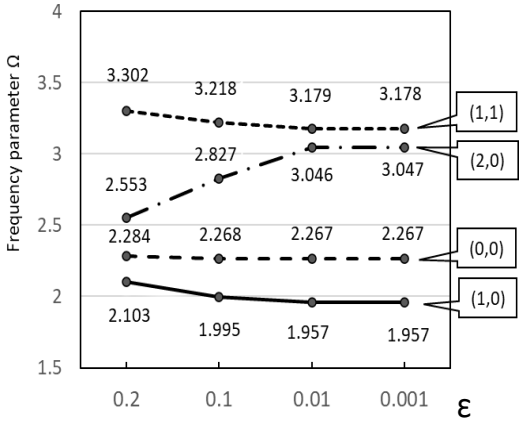
The number of finite elements used in the analysis is forty to give well converged values [10]. In the table, pairs of frequencies obtained from the present Ritz method and the FEM that agree within four significant figures are underlined. Because the plate is completely free, the modes with (n, s) = (0, 0) and (1, 0) correspond to rigid-body motion only and exhibit no elastic deformation.

For ν = 0, the lowest five frequencies correspond to mode shapes in the sequence (n, s) = (2, 0), (1, 1), (0, 1), (3, 0), and (2, 1). As Poisson's ratio increases, the sequence of the third (0, 1) and forth (3, 0) modes is reversed between ν = 0.333 and 0.4, resulting in the sequence (2, 0), (1, 1), (3, 0), (0, 1), and (2, 1) at ν = 0.4 and 0.5. Such changes in frequency sequence due to Poisson's effect are summarized later, together with those of other boundary conditions.

Tables 4 and 5 are presented in the same format as Table 3 and correspond to the S-1 and S-2 type support boundary



(a) S1 supported circular plate



(b) Clamped circular plate

Figure 3. Solid plate approximation by a small hole (ν=0.3)

conditions, respectively. The S-1 plate in Table 4 exhibits no rigid-body motion, whereas the S-2 plate in Table 5 has one rigid-body mode corresponding to in- plane rotation. This distinction is apparent with the constraint conditions of the S-1 and S-2 supports illustrated in Fig. 2.

Table 6 lists the frequency parameters for a totally clamped circular plate in the same format. Since both in-plane displacements *u* and *v* are rigidly constrained to zero along the outer edge, the frequency values are generally higher than the corresponding values reported in the preceding tables. Values in the table can be compared to those of Park [12] and the excellent agreement is found.

As observed from Tables 3–6, the sequence of frequencies changes as Poisson's ratio increases from 0 to 0.5. These variations are illustrated in Fig. 4 for the four boundary conditions. As noted earlier, the (0, 0) and (1, 0) elastic modes do not exist for the free plate in Fig. 4(a), and the (0, 0) mode is also absent for the S-2 plate in Fig. 4(c).

Although the frequency values are strongly dependent on the boundary conditions, it is noteworthy that among the five modes shown in Fig. 4(a)–(d), four modes decrease with increasing Poisson's ratio, while only one mode increases. The increasing modes are the (0, 1) mode in Fig. 4(a), the (0, 0) mode in Fig. 4(b), and the (1, 0) mode in Fig. 4(c). The (0, 1) mode in Fig. 4(d) is only

Table 3 Frequency parameters $\Omega=\omega a\,(\rho(1-\nu^2)/E)^{1/2}$ of "completely free" circular plates.

Poisson's ratio		Nodal circles (s)	Number of nodal diameters (n)					
			0	1	2	3	4	5
ν = 0	Ritz	0	0	0	1.652	2.507	3.232	3.910
	FEM		0	0	1.652	2.507	3.233	3.911
	Ritz	1	1.841	1.750	2.684	3.717	4.791	5.867
	FEM		1.841	1.750	2.684	3.718	4.791	5.868
	Ritz	2	3.631	3.538	4.796	5.868	6.837	7.754
	FEM		3.633	3.539	4.799	5.872	6.841	7.754
ν = 0.1	Ritz	0	0	0	1.570	2.394	3.100	3.760
	FEM		0	0	1.570	2.395	3.101	3.762
	Ritz	1	1.915	1.726	2.659	3.672	4.714	5.755
	FEM		1.916	1.726	2.659	3.672	4.715	5.757
	Ritz	2	3.445	3.538	4.736	5.738	6.649	7.522
	FEM		3.447	3.539	4.739	5.742	6.652	7.520
ν = 0.2	Ritz	0	0	0	1.482	2.269	2.947	3.582
	FEM		0	0	1.482	2.269	2.948	3.584
	Ritz	1	1.984	1.682	2.602	3.584	4.585	5.579
	FEM		1.985	1.682	2.602	3.584	4.586	5.580
	Ritz	2	3.248	3.538	4.655	5.574	6.426	7.259
	FEM		3.250	3.539	4.658	5.579	6.429	7.254
ν = 0.3	Ritz	0	0	0	1.388	2.130	2.774	3.377
	FEM		0	0	1.388	2.131	2.775	3.379
	Ritz	1	2.049	1.618	2.511	3.452	4.401	5.334
	FEM		2.049	1.618	2.512	3.452	4.402	5.336
	Ritz	2	3.038	3.529	4.521	5.349	6.144	6.939
	FEM		3.040	3.530	4.525	5.355	6.147	6.931
ν = 0.333	Ritz	0	0	0	1.355	2.082	2.713	3.304
	FEM		0	0	1.355	2.082	2.714	3.306
	Ritz	1	2.069	1.592	2.474	3.398	4.328	5.239
	FEM		2.069	1.592	2.475	3.399	4.329	5.241
	Ritz	2	2.966	3.519	4.458	5.259	6.036	6.818
	FEM		2.967	3.520	4.462	5.265	6.039	6.808
ν = 0.4	Ritz	0	0	0	1.286	1.978	2.581	3.147
	FEM		0	0	1.286	1.979	2.582	3.149
	Ritz	1	2.109	1.534	2.387	3.274	4.160	5.023
	FEM		2.109	1.534	2.388	3.275	4.161	5.025
	Ritz	2	2.813	3.470	4.298	5.048	5.789	6.542
	FEM		2.814	3.472	4.303	5.055	5.793	6.532
ν = 0.5	Ritz	0	0	0	1.175	1.810	2.366	2.887
	FEM		0	0	1.175	1.811	2.367	2.889
	Ritz	1	2.166	1.429	2.229	3.050	3.861	4.645
	FEM		2.166	1.429	2.229	3.051	3.863	4.648
	Ritz	2	2.568	3.276	3.985	4.670	5.355	6.058
	FEM		2.569	3.279	3.990	4.677	5.360	6.056

Table 4 Frequency parameters $\Omega=\omega a\,(\rho(1-\nu^2)/E)^{1/2}$ of "S1 supported" circular plates.

Poisson's ratio		Nodal circles (s)	Number of nodal diameters (n)					
			0	1	2	3	4	5
ν = 0	Ritz	0	1.841	0.7485	1.676	2.523	3.337	4.133
	FEM		1.841	0.7485	1.677	2.524	3.338	4.134
	Ritz	1	2.709	3.531	4.701	5.630	6.524	7.397
	FEM		2.710	3.531	4.705	5.635	6.530	7.403
	Ritz	2	4.961	3.773	4.948	6.224	7.456	8.656
	FEM		4.965	3.774	4.949	6.225	7.458	8.658
ν = 0.1	Ritz	0	1.915	0.7340	1.602	2.402	3.172	3.926
	FEM		1.916	0.7340	1.602	2.402	3.173	3.927
	Ritz	1	2.570	3.520	4.471	5.345	6.191	7.019
	FEM		2.571	3.521	4.474	5.349	6.197	7.025
	Ritz	2	4.706	3.621	4.958	6.237	7.467	8.666
	FEM		4.710	3.622	4.959	6.238	7.469	8.668
ν = 0.2	Ritz	0	1.984	0.7124	1.521	2.271	2.996	3.705
	FEM		1.985	0.7125	1.521	2.272	2.997	3.706
	Ritz	1	2.423	3.354	4.219	5.041	5.839	6.619
	FEM		2.424	3.356	4.222	5.045	5.844	6.625
	Ritz	2	4.437	3.613	4.975	6.251	7.479	8.673
	FEM		4.441	3.614	4.976	6.253	7.481	8.675
ν = 0.3	Ritz	0	2.049	0.6839	1.432	2.131	2.807	3.470
	FEM		2.049	0.6839	1.432	2.131	2.808	3.471
	Ritz	1	2.267	3.142	3.948	4.717	5.462	6.192
	FEM		2.267	3.144	3.951	4.721	5.468	6.198
	Ritz	2	4.151	3.638	4.994	6.266	7.468	8.308
	FEM		4.154	3.639	4.995	6.268	7.473	8.284
ν = 0.333	Ritz	0	2.069	0.6728	1.401	2.082	2.742	3.388
	FEM		2.069	0.6729	1.401	2.083	2.743	3.389
	Ritz	1	2.213	3.068	3.854	4.604	5.332	6.044
	FEM		2.213	3.069	3.857	4.609	5.338	6.051
	Ritz	2	4.052	3.647	5.001	6.270	7.322	8.111
	FEM		4.055	3.648	5.002	6.272	7.328	8.088
ν = 0.4	Ritz	0	2.099	0.6479	1.334	1.978	2.603	3.216
	FEM		2.099	0.6479	1.334	1.979	2.604	3.217
	Ritz	1	2.109	2.911	3.656	4.367	5.058	5.733
	FEM		2.109	2.912	3.659	4.372	5.063	5.740
	Ritz	2	3.843	3.666	5.014	6.203	6.948	7.694
	FEM		3.846	3.667	5.015	6.213	6.955	7.673
ν = 0.5	Ritz	0	1.916	0.6038	1.224	1.811	2.380	2.938
	FEM		1.916	0.6038	1.225	1.811	2.381	2.940
	Ritz	1	2.166	2.658	3.338	3.987	4.618	5.234
	FEM		2.166	2.659	3.341	3.992	4.623	5.241
	Ritz	2	3.508	3.694	4.974	5.671	6.344	7.025
	FEM		3.511	3.695	4.984	5.680	6.351	7.007

Table 5 Frequency parameters $\Omega=\omega a\,(\rho(1-\nu^2)/E)^{1/2}$ of "S2 supported" circular plates.

Poisson's ratio		Nodal circles (s)	Number of nodal diameters (n)					
			0	1	2	3	4	5
ν = 0	Ritz	0	0	1.191	2.518	3.691	4.789	5.810
	FEM		0	1.191	2.518	3.692	4.789	5.811
	Ritz	1	3.631	2.358	3.428	4.400	5.346	6.310
	FEM		3.633	2.358	3.429	4.402	5.348	6.312
	Ritz	2	3.832	4.749	5.777	6.753	7.699	8.638
	FEM		3.832	4.752	5.783	6.761	7.705	8.623
ν = 0.1	Ritz	0	0	1.239	2.531	3.665	4.687	5.602
	FEM		0	1.239	2.531	3.665	4.688	5.604
	Ritz	1	3.445	2.255	3.287	4.244	5.216	6.239
	FEM		3.447	2.255	3.288	4.246	5.218	6.2396
	Ritz	2	3.832	4.506	5.482	6.408	7.306	8.198
	FEM		3.832	4.510	5.488	6.416	7.312	8.183
ν = 0.2	Ritz	0	0	1.280	2.525	3.583	4.496	5.321
	FEM		0	1.280	2.525	3.583	4.498	5.323
	Ritz	1	3.248	2.150	3.155	4.131	5.159	6.222
	FEM		3.250	2.150	3.156	4.132	5.160	6.223
	Ritz	2	3.832	4.249	5.170	6.043	6.890	7.733
	FEM		3.832	4.253	5.175	6.051	6.896	7.719
ν = 0.3	Ritz	0	0	1.309	2.482	3.429	4.243	4.995
	FEM		0	1.309	2.482	3.430	4.244	4.998
	Ritz	1	3.038	2.046	3.048	4.074	5.145	6.226
	FEM		3.040	2.046	3.048	4.074	5.146	6.226
	Ritz	2	3.832	3.975	4.837	5.655	6.449	7.240
	FEM		3.832	3.979	4.843	5.663	6.455	7.227
ν = 0.333	Ritz	0	0	1.315	2.456	3.364	4.149	4.880
	FEM		0	1.315	2.457	3.365	4.151	4.883
	Ritz	1	2.966	2.013	3.020	4.065	5.145	6.228
	FEM		2.967	2.013	3.021	4.066	5.146	6.228
	Ritz	2	3.832	3.881	4.722	5.521	6.297	7.070
	FEM		3.832	3.884	4.728	5.529	6.303	7.058
ν = 0.4	Ritz	0	0	1.320	2.384	3.214	3.946	4.635
	FEM		0	1.320	2.384	3.215	3.948	4.637
	Ritz	1	2.813	1.948	2.980	4.057	5.148	6.227
	FEM		2.814	1.949	2.980	4.058	5.149	6.227
	Ritz	2	3.832	3.681	4.480	5.238	5.977	6.720
	FEM		3.832	3.684	4.485	5.246	5.983	6.709
ν = 0.5	Ritz	0	0	1.302	2.227	2.955	3.612	4.237
	FEM		0	1.302	2.228	2.956	3.614	4.239
	Ritz	1	2.568	1.866	2.951	4.059	5.142	6.052
	FEM		2.569	1.866	2.952	4.059	5.142	6.043
	Ritz	2	3.832	3.361	4.092	4.788	5.482	6.335
	FEM		3.832	3.364	4.097	4.796	5.489	6.334

Table 6 Frequency parameters $\Omega=\omega a\,(\rho(1-\nu^2)/E)^{1/2}$ of "Clamped" circular plates.

Poisson's ratio		Nodal circles (s)	Number of nodal diameters (n)					
			0	1	2	3	4	5
ν = 0	Ritz	0	2.709	2.075	3.280	4.352	5.345	6.283
	FEM		2.710	2.075	3.281	4.353	5.346	6.285
	Ritz	1	3.832	3.772	4.777	5.768	6.759	7.751
	FEM		3.832	3.773	4.779	5.772	6.764	7.757
	Ritz	2	4.961	5.317	6.607	7.729	8.748	9.720
	FEM		4.965	5.319	6.613	7.739	8.754	9.720
ν = 0.1	Ritz	0	2.570	2.038	3.211	4.241	5.184	6.069
	FEM		2.571	2.038	3.211	4.242	5.186	6.072
	Ritz	1	3.832	3.585	4.556	5.524	6.499	7.477
	FEM		3.832	3.587	4.558	5.528	6.504	7.483
	Ritz	2	4.706	5.299	6.484	7.468	8.403	9.320
	FEM		4.710	5.302	6.492	7.480	8.408	9.316
ν = 0.2	Ritz	0	2.423	1.998	3.134	4.114	4.998	5.822
	FEM		2.424	1.999	3.135	4.115	5.000	5.825
	Ritz	1	3.832	3.388	4.325	5.275	6.238	7.200
	FEM		3.832	3.389	4.328	5.279	6.243	7.207
	Ritz	2	4.437	5.240	6.219	7.108	7.987	8.863
	FEM		4.441	5.244	6.230	7.120	7.991	8.856
ν = 0.3	Ritz	0	2.267	1.957	3.047	3.963	4.777	5.533
	FEM		2.267	1.957	3.048	3.965	4.779	5.536
	Ritz	1	3.832	3.179	4.086	5.024	5.977	6.918
	FEM		3.832	3.180	4.088	5.028	5.982	6.925
	Ritz	2	4.151	5.008	5.859	6.689	7.524	8.367
	FEM		4.154	5.014	5.870	6.702	7.528	8.358
ν = 0.333	Ritz	0	2.213	1.943	3.016	3.906	4.694	5.427
	FEM		2.213	1.943	3.016	3.908	4.697	5.431
	Ritz	1	3.832	3.106	4.005	4.941	5.891	6.822
	FEM		3.832	3.108	4.008	4.945	5.896	6.830
	Ritz	2	4.052	4.900	5.728	6.541	7.362	8.197
	FEM		4.055	4.906	5.739	6.554	7.366	8.187
ν = 0.4	Ritz	0	2.099	1.913	2.944	3.777	4.510	5.195
	FEM		2.099	1.913	2.945	3.779	4.513	5.199
	Ritz	1	3.832	2.955	3.840	4.776	5.714	6.617
	FEM		3.832	2.956	3.843	4.779	5.720	6.625
	Ritz	2	3.843	4.659	5.447	6.227	7.024	7.845
	FEM		3.846	4.665	5.457	6.240	7.028	7.834
ν = 0.5	Ritz	0	1.916	1.863	2.810	3.541	4.187	4.799
	FEM		1.916	1.863	2.811	3.543	4.191	4.803
	Ritz	1	3.508	2.716	3.594	4.533	5.436	6.262
	FEM		3.511	2.717	3.597	4.536	5.443	6.272
	Ritz	2	3.832	4.262	4.991	5.725	6.496	7.318
	FEM		3.832	4.268	5.001	5.737	6.500	7.302

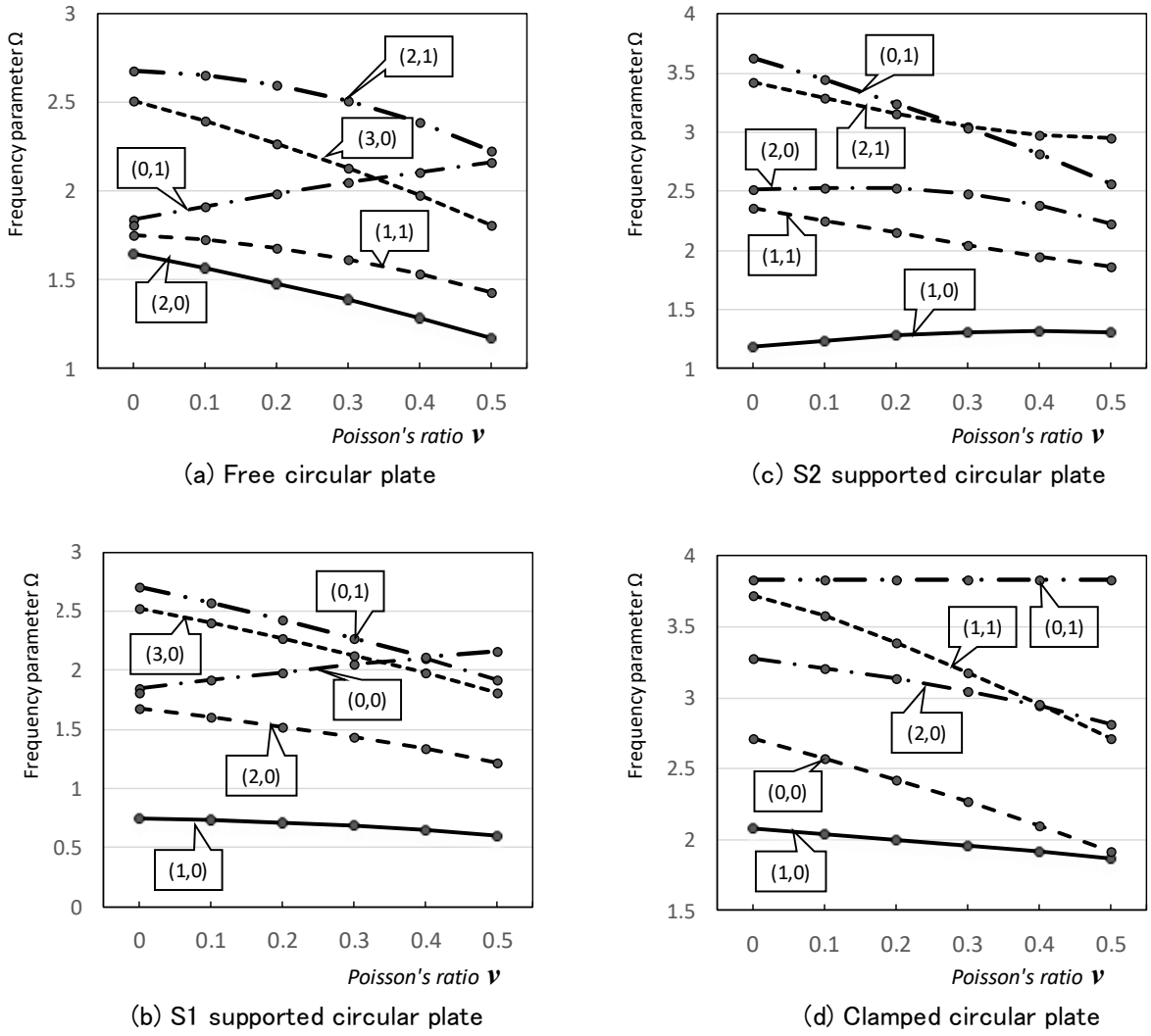


Figure 4. Variations of frequency parameter Ω with Poisson's ratio

weakly affected (i.e., the curve is nearly flat) by changes in Poisson's ratio. It should be also remembered that the frequency parameter Ω contains Poisson's ratio and these comments on the Poisson effects slightly changed when the effect is evaluated by using the radian frequency ω.

4. Conclusions

An analytical approach based on the classical Ritz method was extended to investigate the in-plane free vibration of solid circular plates. The formulation extended a method originally proposed for annular plates to the case of solid circular plates. In addition, a finite-element analysis was implemented by the present author to support the accuracy assessment of the extended Ritz method.

In the numerical study, solution accuracy was examined through convergence test and comparison with results reported by other researchers. In particular, the applicability of the annular-plate formulation to solid plates was evaluated by assuming a very small hole ratio, and it was confirmed that a hole-to-outer-radius ratio of 1/1000 is sufficient to accurately model a solid circular plate with no hole. Frequency parameters were then computed for four in-plane boundary conditions over a wide range of Poisson's ratios. The resulting comprehensive and accurate data are expected to be useful for research comparisons and engineering design applications.

References

[1] Leissa AW. Vibration of Plates, NASA SP-160 (Reprinted in 1993 by the Acoustical Society of America), (1969).

[2] Itao K, Crandall SH, Natural modes and natural frequencies of uniform, circular, free-free plates. J. Applied Mech., 46 (1979), pp.448-453.

[3] Leissa A, Narita Y, Natural frequencies of simply supported circular plates, J. Sound Vibr., 70 (1980), pp.221-229.

[4] Narita Y, Free vibration of elastic plates with various shapes and boundary conditions, Hokkaido University, Doctoral thesis, 1980. https://eprints.lib.hokudai.ac.jp/dspace/handle/2115/32630

[5] Irie T, Yamada G, Muramoto Y, Natural frequencies of in-plane vibration of annular plates. J Sound Vibr. 97 (1984), pp.171-175.

[6] Bashmal S, Bhat R, Rakheha S, In-plane free vibration of circular annular disks, J. Sound Vibr., 322 (2009), pp.216-226.

[7] Ravari MRK, Forouzan MR, Frequency equations for the in-plane vibration of orthotropic circular annular plate, Arch. Appl. Mech., 81 (2011), pp.1307-1322.

[8] Shi X, Shi D, Qin Z, Wang Q, In-plane vibration analysis of annular plates with arbitrary boundary conditions. The Sci World J. (2014).

[9] Wang Q, Shi D, Liang Q, Fazle A, A unified solution for free in-plane vibration of orthotropic circular, annular and sector plates with general boundary conditions, Appl. Math. Model., 40 (2016), pp.9228–9253.

[10] Narita Y, In-plane vibration analysis of annular plates considering all combinations of edge condition, Vibration, 9 (2026). https://doi.org /10.3390/vibration9010017

[11] Farag NH, Pan J, Modal characteristics of in-plane vibration of circular plates clamped at the edge, J. Acoust. Soc. Am. 113 (2003), pp.1935-1946.

[12] Park CI, Frequency equation for the in-plane vibration of a clamped circular plate, J. Sound Vibr., 313 (2008), pp.325-333.

[13] Kim CB, Cho HS, Beom HG, Exact solutions of in-plane natural vibration of a circular plate with outer edge restrained elastically, J Sound Vibr., 331 (2012), pp.2173–2189.